Earth and Planetary Science Letters 432 (2015) 59–72

Contents lists available at ScienceDirect

Earth and Planetary Science Letters

www.elsevier.com/locate/epsl

Modern and long-term evaporation of central Andes surface waters suggests paleo archives underestimate Neogene elevations

Richard P. Fiorella [a,*], Christopher J. Poulsen [a], Ramiro S. Pillco Zolá [b], M. Louise Jeffery [a,d], Todd A. Ehlers [a,c]

[a] Department of Earth and Environmental Sciences, University of Michigan, Ann Arbor, MI 48109, United States
[b] Instituto de Hidráulica e Hidrología, Universidad Mayor de San Andrés, Nuestra Señora de La Paz, Bolivia
[c] Institute of Geosciences, University of Tübingen, Tübingen, Germany
[d] Potsdam Institute for Climate Impact Research, Potsdam, Germany [1]

ARTICLE INFO

Article history:
Received 7 April 2015
Received in revised form 18 September 2015
Accepted 26 September 2015
Available online 3 November 2015
Editor: A. Yin

Keywords:
paleoaltimetry
central Andes
pedogenic carbonate
evaporation
stable isotope geochemistry
water isotopes

ABSTRACT

Central Andean paleoelevations reconstructed from stable isotope and paleofloral data imply a large magnitude (>2 km) Miocene-to-modern surface uplift. However, the isotopic relationships between precipitation, surface waters, and soil waters upon which these reconstructions are based remain poorly constrained for both past, and in many cases, modern conditions. We quantify the relationships between central Andean precipitation and surface waters by measuring the isotopic composition of 249 stream water samples ($\delta^{18}O$ and δD) collected between April 2009 and October 2012. The isotopic compositions of stream waters match precipitation along the eastern flank. In contrast, Altiplano surface waters possess a lower δD–$\delta^{18}O$ slope (4.59 vs ~8 for meteoric waters) not observed in precipitation, which signals heavy isotope evaporative enrichment in surface waters. Paleoclimate models indicate that highly evaporative conditions have persisted on the plateau throughout Andean uplift, and that conditions may have been more evaporative when the Andes were lower. Thus, more ancient proxy materials may have a greater evaporative bias than previously recognized and paleoelevation reconstructions from stable isotope based central Andean plateau proxy materials likely overstate Miocene-to-present surface uplift. We propose Altiplano paleoelevations of 1–2 km at 24.5 Ma, 1.5–2.9 km by 11.45 Ma, and modern elevations by ~6 Ma based on the lightest isotopic compositions observed in Altiplano proxy materials, which are least likely to be influenced by evaporation. These constraints limit total late-Miocene-to-modern uplift to <2.2 km, are more consistent with crustal shortening records, and suggest that plateau uplift may have been more spatially uniform than suggested by previous interpretations of stable isotope proxies.

1. Introduction

Mountain topography is an expression of subsurface tectonic processes and can present significant barriers to atmospheric circulation and biological dispersal. Elevation histories therefore have broad implications for understanding the geodynamic processes that promote orogenesis, reconstructing regional paleoclimates, and discerning spatiotemporal patterns of evolution. Stable isotope paleoaltimetry is one of the few quantitative methods available to reconstruct past elevations. Surface elevations and the stable isotopic composition of precipitation ($\delta^{18}O_p$ and $\delta^{2}H_p$ or δD_p) are related through atmospheric thermodynamics (e.g., Rowley, 2007). Orographic lifting of an airmass results in adiabatic cooling and precipitation, which preferentially removes the heavy isotopes of water relative to the light isotopes (e.g., Rozanski et al., 1993). Progressive rainout along a trajectory leaves the precipitation from an airmass increasingly depleted in heavy isotopes at higher elevations. If surface water isotopic compositions mirror $\delta^{18}O_p$ or δD_p, proxy materials that form in contact with surface waters, such as pedogenic carbonate, authigenic clays, or hydrated volcanic glass, can be used to estimate paleoelevations (Mulch and Chamberlain, 2007; Quade et al., 2007).

In the central Andes, changes in the stable isotope compositions of proxy materials through time have been interpreted to signify >2.0 km of uplift since the early-to-mid Miocene, with variable uplift timing along strike. From north to south, changes in stable

* Corresponding author at: University of Michigan, Department of Earth and Environmental Sciences, 2534 CC Little Building, 1100 N. University Ave., Ann Arbor, MI 48109.
E-mail address: richf@umich.edu (R.P. Fiorella).
[1] Current address.

http://dx.doi.org/10.1016/j.epsl.2015.09.045
0012-821X/

isotope compositions of proxy materials have been taken to reflect uplift of the Altiplano by: (a) 2.2–3.7 km between 19–16 Ma at ∼15°S (Saylor and Horton, 2014), (b) 2.5 ± 1.0 km between 10–6 Ma at ∼18°S (Garzione et al., 2008, 2006), and (c) 2.6 ± 0.7 km between 16–9 Ma at ∼20°S (Garzione et al., 2014). Isotopic compositions from the Salla and Upper Salla Beds in the adjacent Eastern Cordillera at ∼17°S have been interpreted to represent paleoelevations of 0.0–1.5 km at 29–24 Ma, ∼2.5 km at 20–15 Ma, and ∼4 km at 6 Ma (Leier et al., 2013). The spatial and temporal heterogeneity of surface uplift of the central Andean plateau inferred from stable isotope paleoaltimetry appears contrary to observations of broadly synchronous deformation between ∼15–23°S that pre- and postdates the proposed uplift events (Barnes and Ehlers, 2009; Oncken et al., 2006). Deformation began at ∼40 Ma and ceased at ∼10 Ma in the Eastern Cordillera (McQuarrie, 2002; McQuarrie et al., 2005), and propagated into the Bolivian Altiplano at ∼30 Ma and ceased by ∼7 Ma (Elger et al., 2005; Lamb and Hoke, 1997). Therefore, if these paleoelevation constraints are accurate, the uplift mechanism must allow for a substantial amount of surface uplift from processes other than crustal thickening (e.g., via lithospheric mantle removal), and accommodate several million years of deformation without producing significant uplift.

Paleoclimate model simulations of Andean uplift challenge the assertion that isotopic changes in these proxy materials primarily record changes in surface elevation. Climate changes attendant to Andean uplift contribute to and may dominate the isotopic signal observed in proxy materials. These changes include an increase in precipitation rate, an intensification of convective precipitation, and a shift from in vapor source for the central Andes from primarily Pacific to Atlantic dominated (Ehlers and Poulsen, 2009; Poulsen et al., 2010). Abrupt, large (∼5–6‰ in $\delta^{18}O_p$) isotopic changes occur when the Andes reach a threshold of 70–75% of their modern elevation, suggesting large isotopic change can occur in the absence of significant uplift (Insel et al., 2012; Poulsen et al., 2010). Climate model simulations have generally used a simplified model of Andean uplift, where elevations are scaled as percentages of their modern elevation across the entire orogen. Despite their simplistic representation of uplift, these simulations demonstrate that uplift strongly alters continental climate and regional $\delta^{18}O_p$, and challenge the interpretation that proxy materials primarily record rapid surface uplift.

However, both the proxy and model based paleoaltimetry studies have assumed that changes in precipitation $\delta^{18}O$ or δD are fully reflected in proxy $\delta^{18}O$ or δD. This assumption may not be universally valid, as proxy materials ultimately acquire their isotopic composition from surface waters (e.g., in soils or streams) and not directly from precipitation. Stream waters reflect a spatially and temporally integrated signal of precipitation composition, and proxy materials forming in contact with these waters would therefore record the integrated composition of catchment precipitation. However, in arid regions, evaporation may enrich surface waters in heavy stable isotopes (e.g., Kendall and Coplen, 2001), and will undermine the relationship between elevation and $\delta^{18}O$ or δD.

The relationship between precipitation and surface water isotope compositions across the central Andes is poorly known due to temporally and spatially limited observations. One transect across the eastern Andes flank (∼16°S) indicates a close match between stream water and precipitation $\delta^{18}O$ (Bershaw et al., 2010), but this relationship may not hold across the strong climate and elevation gradients of the central Andes (e.g., Garreaud et al., 2003). Critically, until now, no stream water data were available for the central plateau to evaluate their relationship to precipitation. To assess whether surface waters reflect precipitation across the central Andes (∼17–22°S), we measured the isotopic compositions of 249 streams distributed across the Altiplano and its eastern flank. We then compared them to published values of regional precipitation $\delta^{18}O$ (Fig. 1) (Aravena et al., 1999; Fiorella et al., 2015; Gonfiantini et al., 2001). We find that evaporation biases the isotopic composition of streams on the central Andean plateau to heavier isotope ratios than precipitation. In contrast, streams along the eastern flank generally do not exhibit this evaporative bias. If these heavier isotopic values across the plateau were preserved in proxy materials, the records would be interpreted to reflect elevations that are too low. Paleoclimate model simulations of Andean uplift indicate that regional conditions were more evaporative when elevations were lower, raising the concern that greater bias in older proxy materials has led to overestimations of Neogene uplift. Finally, we note that this interpretation of the stable isotope proxy record may resolve some of the controversy in uplift rates and magnitudes apparent across different approaches applied to the central Andes, and suggests that Andean plateau uplift may have been more synchronous than it may appear from stable isotope proxy records.

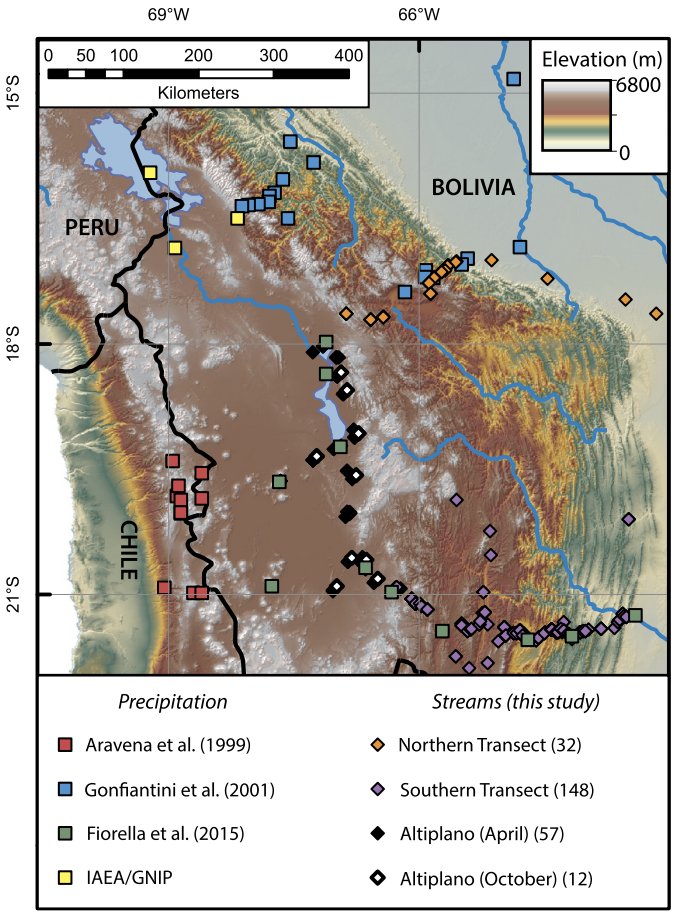

Fig. 1. Geographic overview of compiled isotopic composition of precipitation (colored squares) and stream waters collected for this study (colored diamonds). Streams were collected in three separate physiographic regions: two elevation transects at ∼17°S (orange diamonds) and ∼21°S (purple diamonds), and streams entirely within the Altiplano (white diamonds were collected in April, black diamonds in October). Elevation data are from the ASTER DEM product (METI and NASA).

2. Methods

2.1. Stream water collection and analysis

We collected annual stream water samples across the Bolivian Altiplano and along two transects of its eastern flank (at ∼17.5°S and ∼21.5°S, Fig. 1). Stream samples for the Altiplano and the southern transect were collected from April 2009 until

May 2012; the northern transect was added in April 2010 and collected until May 2012. We also collected 12 stream samples in October 2012 to determine the seasonal variability of Altiplano surface waters. We measured isotopic compositions using a Picarro L2120-i Cavity Ringdown Spectrometer coupled to an A0211 high precision vaporizer and autosampler. Compositions are reported in delta notation as per mil deviations from VSMOW ($\delta = 1000(R_{sample}/R_{VSMOW} - 1)$, where R is the heavy to light isotope ratio) (Coplen, 1996). Standard error is ~0.1‰ for $\delta^{18}O$ and ~0.4‰ for δD. For clarity in the following discussion, isotopic compositions of precipitation, surface waters, and pedogenic calcite are designated as δ_p, δ_w, or δ_{cc} respectively.

We calculated hypsometric mean catchment elevation and drainage areas using the Advanced Spaceborne Thermal Emission and Reflection Radiometer (ASTER, v.2) global digital elevation model (30 m resolution) (METI and NASA) and GIS software (ArcGIS 10). Stream sampling locations ranged from 230 m to 4430 m, corresponding to mean catchment elevations of 319 m to 4499 m. Catchment areas range from <1 km^2 to 61,840 km^2, with a median area of 12.1 km^2. Detailed isotopic and elevation calculation methods are available as supplemental information. Stream water isotopic compositions, catchment elevations, and sampling dates are presented in Table S1.

2.2. Prediction of catchment elevations from isotopic composition

We compare hypsometric mean elevations to predicted elevations from two different isotope-elevation models. First, we predicted elevations using a semi-empirical thermodynamic model that extracts low-latitude surface temperature and relative humidity over the oceans from reanalysis data to generate relationships between isotopic composition, condensation amount, and surface elevation (Rowley, 2007). The amount of condensate removed from an air parcel with increasing elevation is determined by the moist adiabat above the elevation where condensation begins. If all the condensate is removed as precipitation, δ_p follows Rayleigh fractionation (e.g., Rozanski et al., 1993), and the difference in δ_p from its value at sea level is directly related to elevation. Where it reflects δ_p, δ_w follows the same relationship if catchment δ_p is also weighted hypsometrically. We use the quartic regression of Rowley (2007, equation (5)) to estimate the hypsometric mean catchment elevations based on their isotopic compositions:

$$z_{\text{weighted mean}} = -0.0129\Delta(\delta^{18}O)^4 - 1.121\Delta(\delta^{18}O)^3 - 38.214\Delta(\delta^{18}O)^2 - 715.22\Delta(\delta^{18}O)$$

where $\Delta(\delta^{18}O)$ refers to the difference in $\delta^{18}O$ from its initial low-elevation value. We estimate initial δ_w values of −6.0‰ and −4.0‰ for streams sampled north and south of 20°S respectively, based on observations of low-elevation δ_p and δ_w (Fiorella et al., 2015; Gonfiantini et al., 2001). This division both separates the two flank transects, and reflects differences in vapor transport to the northern and southern Altiplano (e.g., Fiorella et al., 2015).

Second, we predicted catchment elevations using a linear regression between isotopic composition and elevation. Following the same logic employed for the semi-empirical thermodynamic model above, two separate linear regressions were produced for the northern and southern transect catchments to match observations of vapor transport to the Altiplano. We calculate a best-fit linear equation for the northern transect of (uncertainty on coefficients is 1σ):

$$\text{elev(m)} = -500.1 \pm 73.0\delta^{18}O - 2849.6 \pm 838.8$$
$$(r^2 = 0.61, 2\sigma \text{ prediction int.} = 2000 \text{ m})$$

and for the southern transect of:

$$\text{elev(m)} = -358.5 \pm 23.9\delta^{18}O - 477.1 \pm 214.1$$
$$(r^2 = 0.61, 2\sigma \text{ prediction int.} = 1420 \text{ m})$$

We predicted mean catchment elevations for all samples north (south) of 20°S with the northern (southern) transect equation. To assess whether our results were sensitive to the choice of linear model, we also calculated several alternate linear models based on different divisions of our stream dataset. We restricted our candidate models to those that account for the direction of vapor transport to the Altiplano. All alternate models exhibited a weaker fit based on r^2 and AIC values (Table S2). The general conclusions from our analysis are not sensitive to the choice of linear model when vapor source direction is accounted for (Figs. S1 and S2).

For both the empirical and semi-empirical thermodynamic model predictions, we then calculated the residual between model predictions and GIS-derived elevations for each catchment. Where model predictions match measured elevations, the residual should approach zero.

2.3. Paleoclimate model simulations of Andean uplift

Central Andean precipitation and evapotranspiration fluxes were evaluated throughout uplift using the climate modeling experiments of Ehlers and Poulsen (2009). In these simulations, the elevation of the Andes is varied in 25% increments relative to modern in the Regional Climate Model (RegCM), version 3 (Pal et al., 2007). The horizontal resolution used in these simulations is ~60 km, which provides more realistic representation of Andean topography than typical resolutions for global models (>100 km). All other boundary conditions are specified at modern values to isolate the effect of topographic changes on continental climate.

We use model-derived monthly precipitation and evapotranspiration fluxes to constrain seasons of pedogenic carbonate formation. Pedogenic carbonates form when dissolved calcium ion concentrations are high and soil CO_2 concentrations are low, both of which occur when soils lose water (Breecker et al., 2009). Thus, we highlight months where evapotranspiration exceeds precipitation as periods of carbonate formation.

3. Results

3.1. Stream water isotopic compositions

Stream waters along both elevation transects are more depleted in heavy isotopes at high elevations than at low elevations (Fig. 2). Isotopic compositions on the northern transect range from −6.56‰ (−41.62‰) to −14.86‰ (−110.87‰) for $\delta^{18}O_w$ (δD_w), and correspond to measured mean catchment elevations of 380 and 4499 m respectively. Isotopic compositions along the southern transect range from −1.77‰ (−24.25‰) to −15.82‰ (−112.89‰) for $\delta^{18}O_w$ (δD_w), and correspond to mean catchment elevations of 2300 and 4050 m, respectively. Stream water compositions exhibit a larger isotopic range on the Altiplano than on the eastern flanks (Fig. 2). Altiplano $\delta^{18}O_w$ (δD_w) values vary from 5.44‰ (−18.73‰) to −16.38‰ (−123.60‰). Both extreme values for the Altiplano occur in catchments with mean elevations exceeding 3800 m.

Multivariate least-squares linear regression (see SI for methods) between $\delta^{18}O_w$ and geographic variables indicates significant ($p < 0.05$) associations of $\delta^{18}O_w$ with elevation and sampling latitude across all sampled streams (Table S3). A similar best model emerges when only flank catchments are considered (Table S4). When only Altiplano stream $\delta^{18}O_w$ is considered, the best model retains elevation and annual precipitation, but not latitude, as predictor variables (Table S5). However, the preferred model for Altiplano $\delta^{18}O_w$ only describes a small portion of the observed variance ($r^2 = 0.322$).

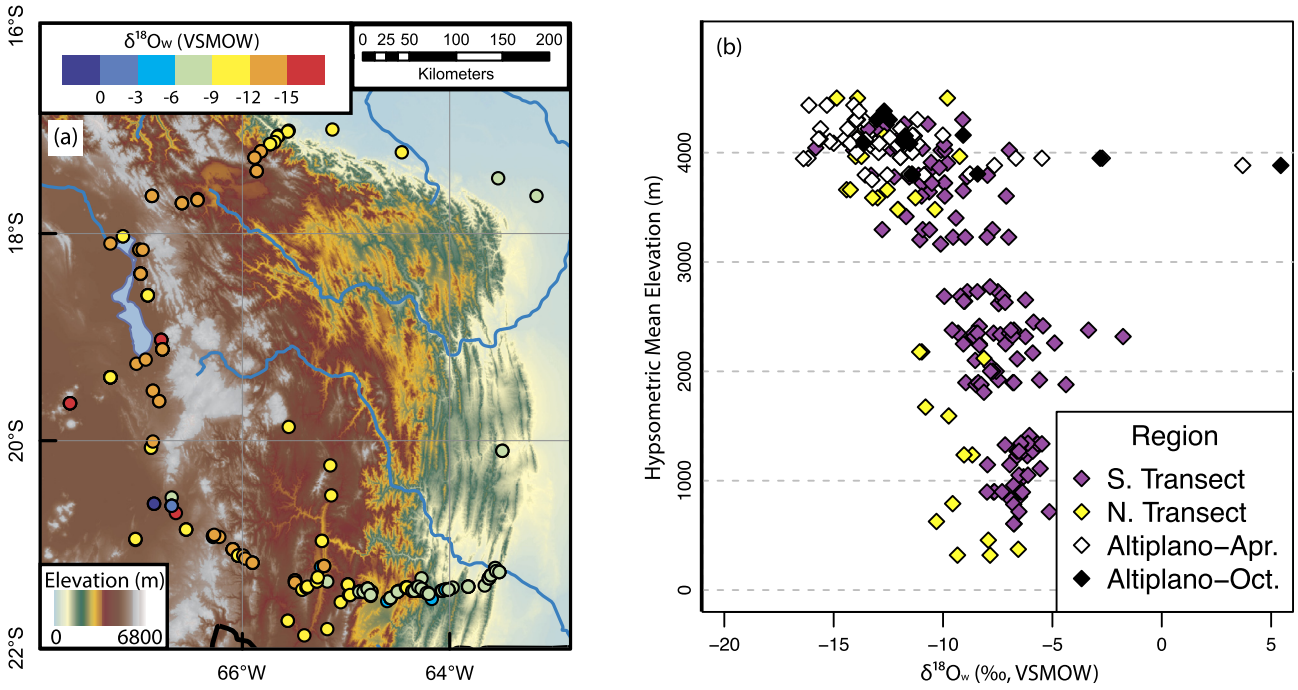

Fig. 2. Spatial distribution of the $\delta^{18}O_w$ of central Andes stream waters. (a) Map view of collected stream waters. Colored circles denote each stream sample, with blue (red) indicating the compositions least (most) depleted in ^{18}O. (b) Scatter plot of $\delta^{18}O_w$ of central Andes stream waters versus hypsometric mean elevation (m). Higher elevation catchments tend to have more negative isotopic compositions for elevations below 3500 m. On the Altiplano above 3500 m, however, compositions are more variable. Standard errors for $\delta^{18}O_w$ are ~0.1‰.

3.2. Isotopic lapse rates and elevation catchment predictions

Isotopic lapse rates along the two transects, determined by univariate linear regression, differ from year to year (Table 1). Northern transect $\delta^{18}O_w$ lapse rates vary from -0.79 ± 0.31‰/km in 2010 to -1.66 ± 0.16‰/km in 2011. Southern transect $\delta^{18}O_w$ lapse rates are generally larger in magnitude, and vary from -1.52 ± 0.32‰/km in 2010 to and -1.77 ± 0.14‰/km in 2012. Other portions of the eastern Andean flank exhibit similar isotopic lapse rates in both stream waters and precipitation, though all archives exhibit substantial interannual variability (Table 1) (Bershaw et al., 2010; Fiorella et al., 2015; Gonfiantini et al., 2001; Rohrmann et al., 2014).

GIS-derived mean catchment elevations were compared to predictions from δ_w using two models of the isotope-elevation relationship. Both the semi-empirical thermodynamic model (Rowley, 2007) and locally calculated empirical linear regressions produce overestimates of the true elevation of low-elevation (<2000 m) catchments, and both models also underestimate the true elevation of high-elevation catchments for both the northern and southern transects (Fig. 3a–d), similar to observations further north in the Eastern Cordillera (Saylor et al., 2009). For the semi-empirical thermodynamic model, this pattern is more pronounced in the northern transect than in the southern transect. Half of the predictions from catchments below 1000 m in the northern transect overestimate their true elevation by more than 1000 m, and all ten of the predicted elevations for catchments below 2000 m are higher than their actual elevation (Fig. 3c). The linear empirical model produces a similar trend in the residuals that is approximately equal for both transects (Fig. 3d). At high elevations, model predictions tend to underestimate measured elevations, most notably on the plateau (Fig. 3a–d).

Model predicted elevations appear to perform well along the flanks when considered as a distribution. For the Rowley (2007) model, the mean residuals between predicted and observed catchment elevations are 20 m and −140 m for the northern and southern transects respectively, and the most frequent values inferred from the distributions are both within ±200 m of zero (Fig. 3e). The mean residual for the flank distributions in both linear regression models is ~0 m. Distribution mean residuals for both models are low on the flanks, with overestimations at low elevations are counterbalanced by underestimations at high elevations, resulting in distributions that appear normal and are centered near zero. In contrast, residuals for Altiplano streams are skewed toward negative values, with several predictions underestimating measured catchment elevations by >2.0 km (Fig. 3e, f). For both models, substantially more than half of the elevation predictions for Altiplano catchments have residuals below zero (79% Rowley, 65% linear empirical), indicating that Altiplano catchment elevations are poorly described by both models.

3.3. Central Andes precipitation and evapotranspiration rates through uplift

When the Andes are low (0–25% of modern elevations), RegCM simulations estimate a higher evapotranspiration to precipitation (E/P) ratio in the central Andes, and thus more arid conditions (Fig. 4a, b) (Ehlers and Poulsen, 2009). In contrast, when the Andes exceed 50% of their modern elevations, regional aridity decreases, most markedly along the flanks (Fig. 4c, d, e). Predicted precipitation rates for the Altiplano region (defined as the 126 grid cells within the red polygon in Fig. 4a–e, after Isacks, 1988; McQuarrie et al., 2005) increase from 0.86 mm/day at 0% of modern elevations to 6.61 mm/day at 100% of modern elevations (Fig. 4f). Evapotranspiration rates also increase during Andean uplift, but not at every stage. Mean evapotranspiration rates more than triple between 0% (0.78 mm/day) and 75% of modern elevations (2.85 mm/day) (Fig. 4g). Increased water availability from additional precipitation and an increase in shortwave radiation associated with a higher elevation surface fuels the higher evapotranspiration rates. Continued uplift above 75% of modern elevations decreases evapotranspiration rates slightly (to 2.62 mm/day,

Table 1
Compilation of central Andes eastern flank isotopic lapse rates.

Stream waters

Latitude	Year	Mean catchment elevation range (m)	Sample count	$\delta^{18}O$ lapse rate (‰/km)	Reference
15°S	2004	829–4683[a]	36	−1.90 ± 0.08	Bershaw et al. (2010)
15°S	2005	408–4823[a]	46	−1.53 ± 0.06	Bershaw et al. (2010)
15°S	**all**	**408–4823**[a]	**82**	**−1.67 ± 0.05**	**Bershaw et al. (2010)**
17.5°S	2010	456–4499	9[b]	−0.79 ± 0.31	this study
17.5°S	2011	319–4499	10[b]	−1.66 ± 0.16	this study
17.5°S	2012	319–4499	11[b]	−1.24 ± 0.11	this study
17.5°S	**all**	**319–4499**	**30**[b]	**−1.15 ± 0.18**	**this study**
21°S	2009	784–4301	45[b]	−1.76 ± 0.18	this study
21°S	2010	895–4261	29[b]	−1.52 ± 0.32	this study
21°S	2011	373–4116	33[b]	−1.69 ± 0.14	this study
21°S	2012	606–4261	43[b]	−1.77 ± 0.14	this study
21°S	**all**	**373–4301**	**150**[b]	**−1.67 ± 0.11**	**this study**
22–24°S	2010	701–4416	14[c]	−1.93 ± 0.34	Rohrmann et al. (2014)
22–24°S	2011	3069–4197	11	−0.23 ± 0.63	Rohrmann et al. (2014)
22–24°S	2012	3623–4013	7	−5.46 ± 1.21	Rohrmann et al. (2014)
22–24°S	2013	625–4326	17	−1.35 ± 0.27	Rohrmann et al. (2014)
22–24°S	**all**	**625–4416**	**49**	**−1.69 ± 0.17**	**Rohrmann et al. (2014)**
24–26°S	2010	1236–4587	11	−0.23 ± 0.29	Rohrmann et al. (2014)
24–26°S	2011	1856–4006	12	−0.63 ± 0.68	Rohrmann et al. (2014)
24–26°S	2012	1112–4836	77	−1.09 ± 0.12	Rohrmann et al. (2014)
24–26°S	**all**	**1112–4836**	**100**	**−0.88 ± 0.12**	**Rohrmann et al. (2014)**
26–28°S	2011	340–4437	83	−0.21 ± 0.09	Rohrmann et al. (2014)
26–28°S	2012	1647–3764	4	0.14 ± 0.69	Rohrmann et al. (2014)
26–28°S	**all**	**340–4437**	**87**	**−0.21 ± 0.09**	**Rohrmann et al. (2014)**

Precipitation samples

Latitude	Year	Station elevation range (m)	Number of stations	$\delta^{18}O$ lapse rate (‰/km)	Reference
15°S	1983	200–5200	12	−1.5 ± 0.2	Gonfiantini et al. (2001)
15°S	1984	200–5200	12	−2.4 ± 0.2	Gonfiantini et al. (2001)
17.5°S	1985	405–3220	7	−1.6 ± 0.2	Gonfiantini et al. (2001)
21°S	2008[d]	395–4340	5	−1.2 ± 0.8	Fiorella et al. (2015)
21°S	2009	395–4340	5	−2.0 ± 0.3	Fiorella et al. (2015)
21°S	2010	395–4340	5	−2.2 ± 0.2	Fiorella et al. (2015)
21°S	2011[e]	395–4340	5	−1.3 ± 0.4	Fiorella et al. (2015)

[a] Published elevations were given as sampling elevations, not mean catchment elevations.
[b] Includes only flank catchments that are not within the internally-drained Altiplano.
[c] Sample W10-PUR02 removed from regression due to excessive evaporation, as in Rohrmann et al. (2014).
[d] Precipitation samples collected from September–December only.
[e] Precipitation samples collected from January–September only.

Fig. 4g), which is consistent with lower surface temperatures and higher relative humidity. Together, these trends indicate that the average E/P ratio decreases in the region throughout uplift, but also becomes more spatially variable as shown by the increasing range of values (Fig. 4h).

4. Interpretation of the modern δ_w distribution

Elevation provides a dominant control on central Andes $\delta^{18}O_p$ (Fiorella et al., 2015; Gonfiantini et al., 2001). Stream water $\delta^{18}O$ compositions generally preserve the relationship between $\delta^{18}O_p$ and elevation along the flanks (Fig. 5a, b), while on the Altiplano we observe substantial variability in $\delta^{18}O_w$ not observed in $\delta^{18}O_p$ (Fig. 5c). The spread in Altiplano δ_w cannot be explained by catchment elevations, as both extreme values occur in catchments with mean measured elevations of >3800 m. Instead, these trends imply that different processes govern the isotopic composition of surface waters on the Altiplano compared to its eastern flank.

To investigate this possibility, we compare the $\delta^{18}O_w$–δD_w relationship of flank and Altiplano streams to the $\delta^{18}O_p$–δD_p relationship for published precipitation values (Aravena et al., 1999; Fiorella et al., 2015; Gonfiantini et al., 2001) (Fig. 6). The $\delta^{18}O$–δD relationship reflects the integrated condensation and evaporation history of the water pool, and the Altiplano $\delta^{18}O_w$–δD_w relationship should differ from the flanks if different processes control the isotope distribution in the two regions. Regional precipitation shows a consistent $\delta^{18}O_p$–δD_p relationship (Fig. 6a) that falls along the global meteoric water line (GMWL, black line in each panel of Fig. 6) (Rozanski et al., 1993). Transect δ_w values also follow the GMWL (Fig. 6b); however, Altiplano δ_w values follow a distinctly shallower slope (Fig. 6c, slope = 4.59 ± 0.11), which is consistent with evaporation of Altiplano surface waters. Evaporation also decreases the deuterium excess of natural waters (d-excess = δD-8$\delta^{18}O$), as kinetic fractionation during evaporation results in a stronger fractionation between ^{18}O and ^{16}O relative to that between D and H (e.g., Rozanski et al., 1993). The global average d-excess in precipitation implied by the GMWL is ~10 (Rozanski et al., 1993), though d-excess in central Andes precipitation has been observed to range between 14–20 (Fiorella et al., 2015; Gonfiantini et al., 2001). If we characterize any stream water sample with a d-excess value below 5 as evaporated, 68% of Altiplano stream samples exhibit evaporation (April only, 74% including October samples), compared to only 13% of catchments along both elevation transects. Evaporation does not appear to occur during precipitation as a subcloud process (e.g., Rohrmann et al., 2014), as Altiplano precipitation does not have low d-excess values compara-

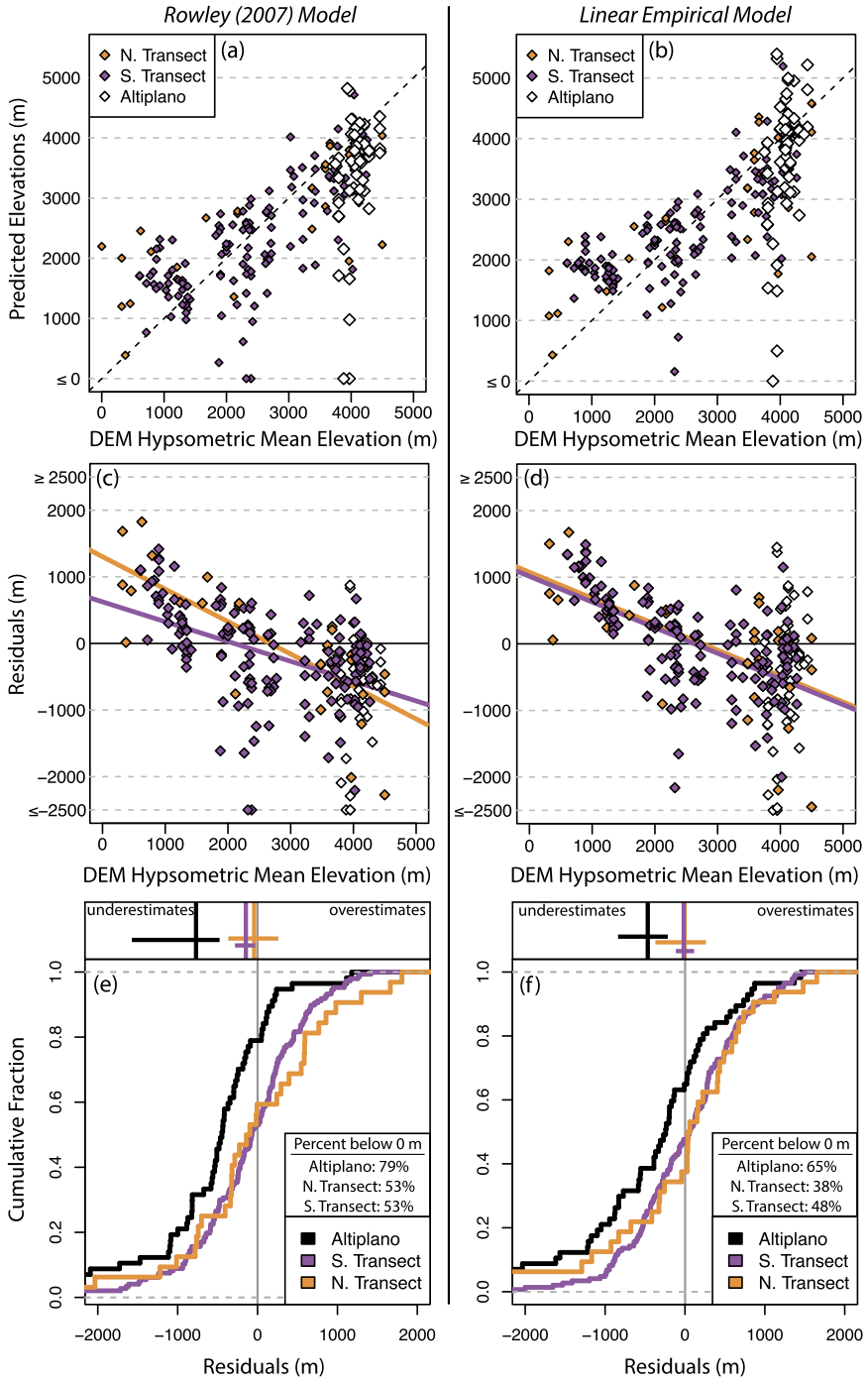

Fig. 3. Comparison of measured and model predicted catchment elevations for the Rowley semi-empirical thermodynamic model (2007, left column) and a linear empirical model (right column). (a, b) Direct comparison between predicted and measured elevations by physiographic region. Elevation predictions deviate from model expectations by >3000 m at several of the highest elevation Altiplano catchments. (c, d) Residual between prediction and measurement. The best-fit line is plotted for the north (orange) and south (purple) transects. (e, f) Empirical cumulative distribution functions of residuals between predicted and measured elevations. Residuals for the two elevation transects are both normally distributed and centered around zero. Stream waters on the Altiplano, however, are consistently biased to predict lower-than-observed elevations, and skewed toward multi-kilometer underestimation and away from overestimation. Distribution mean values are shown as vertical lines above the distributions, and 95% confidence intervals based on 50,000 bootstrap replicates with replacement are shown as horizontal lines. (For interpretation of the references to color in this figure legend, the reader is referred to the web version of this article.)

ble to the stream waters (Fiorella et al., 2015). Therefore, evaporation of surface waters must occur following rainout, promoting the different $\delta^{18}O$–δD relationship observed between Altiplano precipitation and stream waters.

Evaporation of Altiplano surface waters biases model predictions to lower elevations, and is responsible for the biased distribution observed (Fig. 3e, f). The most evaporated Altiplano stream waters, which have the heaviest compositions, yield elevation predictions that are below sea level (Fig. 3a, b). These predictions clearly demonstrate the potential of evaporation to impair elevation estimates. Though the most frequently observed Altiplano residuals occur between −250 and −750 m, the influence of the most evaporated streams lowers the mean Altiplano residual to −840 m for the Rowley model (Fig. 3e), and −460 m for the lin-

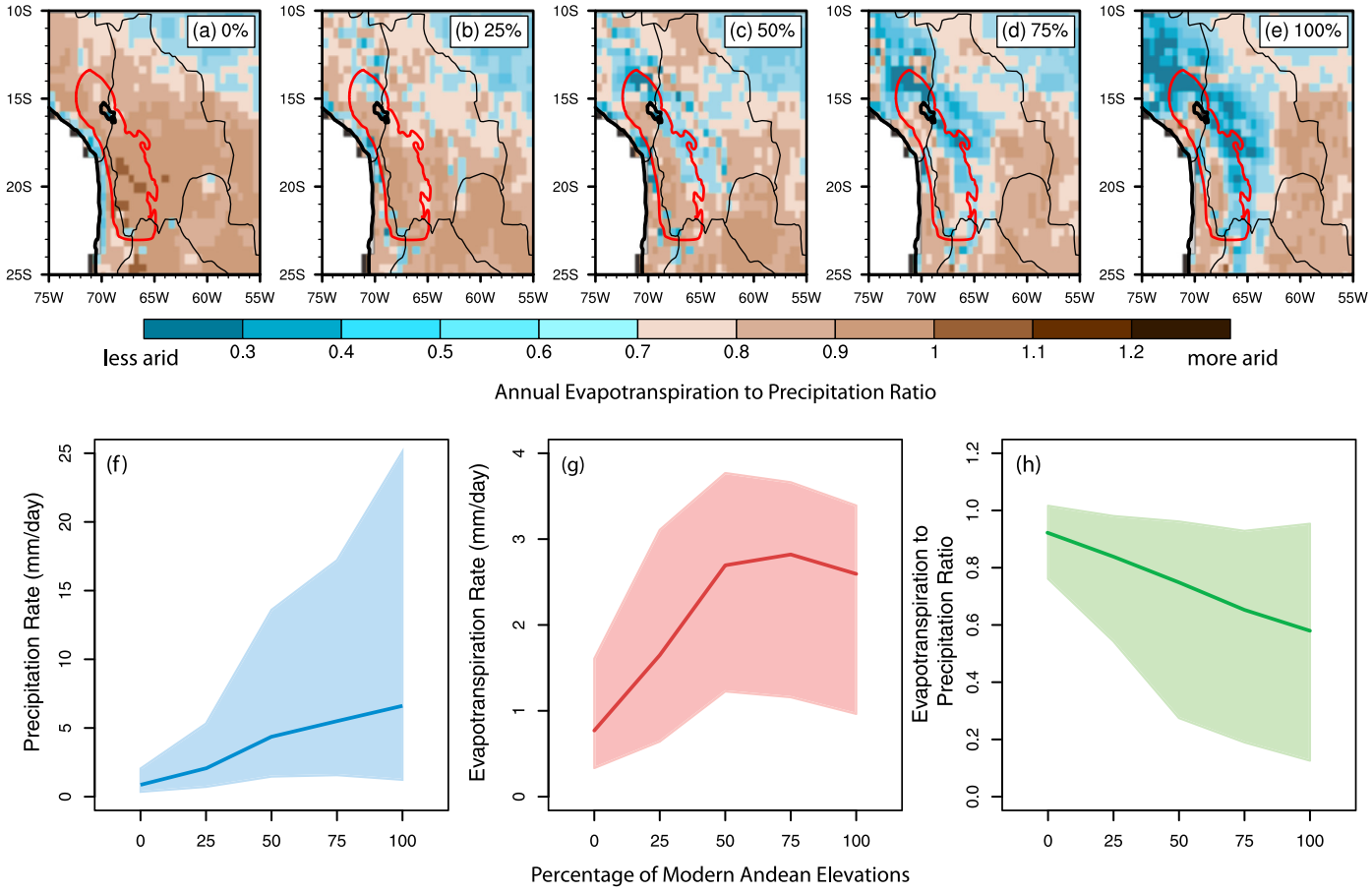

Fig. 4. Climate model predicted regional mean precipitation and evapotranspiration rates through Andean uplift. (a)–(e) Evapotranspiration to precipitation ratio across the central Andes region, with elevations increasing from 0% to modern in 25% increments from (a) to (e). Higher values (shown as progressively more brown) indicate increasingly arid conditions. Throughout uplift, the central Andes region becomes progressively less arid throughout uplift, but with stronger spatial gradients effected by topography. Annual precipitation (mm/day) (f), evapotranspiration (mm/day) (g), and evapotranspiration to precipitation ratio (unitless) (h) are also shown, with the range shown for all the model grid cells in the Altiplano region (defined as red outlined area in (a)–(e)). Areal mean values are shown as a heavy line in (f)–(h), and 2σ variability indicated by the shaded polygon. Andean uplift results in increases in both precipitation and evapotranspiration, but a decrease in the evapotranspiration to precipitation ratio as precipitation rates increase by a greater amount. (For interpretation of the references to color in this figure legend, the reader is referred to the web version of this article.)

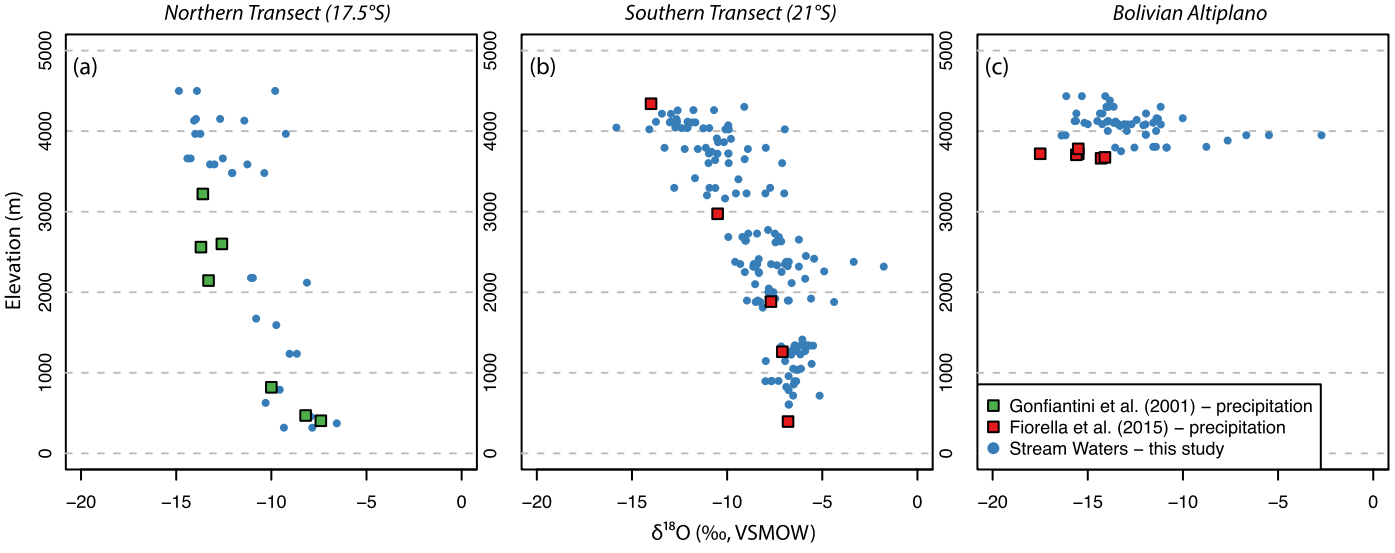

Fig. 5. Scatter plots of the isotopic composition of precipitation and stream waters compared to elevation along the northern transect (a), southern transect (b), and Altiplano (c) regions. Precipitation compositions are plotted at the station elevation, while stream elevations are plotted as catchment mean elevations. Precipitation and stream water samples show similar relationships between $\delta^{18}O$ and elevation along the flanks (a and b), but show different relationships on the Altiplano (c) due to evaporative enrichment of the heavy isotopes in stream waters that is not observed in precipitation.

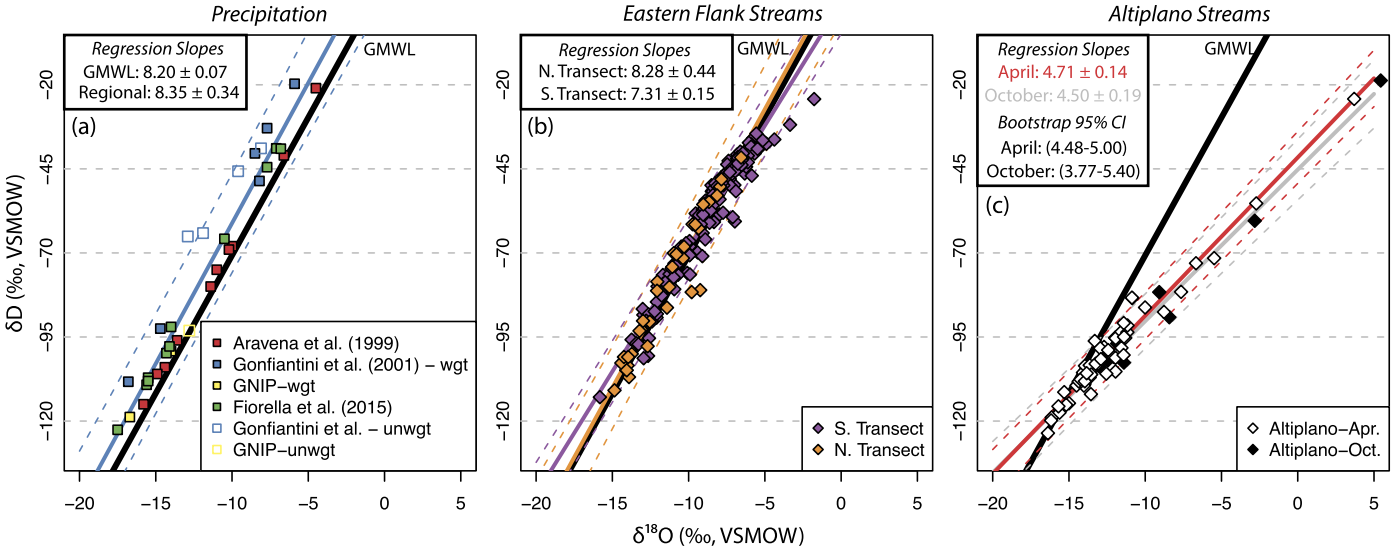

Fig. 6. δD versus δ^{18}O for compiled precipitation data (a), streams along the eastern flank (b), and streams contained within the Altiplano (c). The Global Meteoric Water Line (GMWL, Rozanski et al., 1993) is plotted in (a)–(c) for reference and represents a global composite of the δD–δ^{18}O relationship for precipitation. In (a), filled symbols represent precipitation amount-weighted averages. Open symbols represent stations where precipitation measurements were not available; thus, these represent unweighted averages of delta values. Regression slope and uncertainties (2σ) are shown in the inset, and the best-fit line and 2-sigma prediction interval is plotted for each region and water type. For (c), 95% confidence intervals of the slope are calculated separately for April and October using 50,000 bootstrap replicates with replacement. Precipitation (a) and flank stream (b) compositions plot closely to the GMWL, while streams on the Altiplano (c) follow a lower slope line (shown in red for April, gray for October). This lower slope line is characteristic of evaporation. (For interpretation of the references to color in this figure legend, the reader is referred to the web version of this article.)

ear empirical model (Fig. 3f). In contrast, since evaporation is only observed in a small fraction of samples along the flank, these distributions are not systematically biased toward lower elevations (Fig. 3e, f). However, a trend in the residuals along the flank remains (Fig. 3c, d), where low (high) elevation catchments tend to have elevation predictions that are too high (low). We note two potential reasons for this relationship. First, prior climate modeling experiments have suggested that the isotopic lapse rate is not linear for all elevations, and varies in time and space due to variability in convective precipitation and entrainment of vapor from multiple vertical levels in the atmosphere (Insel et al., 2012). Second, low-elevation isotopic compositions at the eastern Andean flank are highly variable from year-to-year, and are closely related to convective and precipitation intensity over the Amazon Basin (e.g., Fiorella et al., 2015). Regardless, only the plateau catchments show substantial evidence of evaporation (Fig. 6), lower d-excess values, higher δD_w and $\delta^{18}O_w$ values than anticipated for their elevation (Figs. 5–6), and ultimately, a physical basis for elevation underestimation.

We find limited evidence for other potential explanations for the spatial pattern of evaporation on the plateau. For example, relationships between Altiplano $\delta^{18}O_w$ and catchment area ($r^2 = 0.02$), latitude ($r^2 = 0.16$), and longitude ($r^2 = 0.01$) are weak; thus, basin size and position are unlikely explanations for variability on the Altiplano (Table S5). Furthermore, the lower slope observed for Altiplano surface waters does not result from a few highly influential evaporated streams. Resampling of the Altiplano stream waters to remove the ten most evaporated streams yields a slope of 5.35 ± 0.25 (compared to 4.59 ± 0.11 with all streams), which is still much lower than the anticipated value of $\sim$8 for unevaporated meteoric waters. Wide isotopic variations in Altiplano surface waters indicate variability in evaporative intensity. For example, the most evaporated surface waters exhibit isotopic compositions heavier than measured Altiplano $\delta^{18}O_p$ by $>10‰$ (Fiorella et al., 2015), while stream waters that are less affected by evaporation may have isotopic compositions within 1‰ of $\delta^{18}O_p$.

5. Discussion

5.1. Evaporative imprint on proxy materials and elevation reconstructions

Spatially variable evaporative intensity on the plateau provides the most direct explanation for the large range of Altiplano δ_w and the lower slope δ^{18}O–δD relationship. The occurrence of large salt flats, such as the *Salar de Uyuni*, provide evidence for significant evaporation on the modern Altiplano. If evaporated surface waters propagate to proxy bearing soil horizons, proxies forming in equilibrium with these soil waters will record compositions heavier than precipitation. Interpretations from these proxy materials will be prone to underestimate elevation because of the heavier compositions recorded. Therefore, we consider lighter isotopic compositions to be stronger evidence for high elevations than heavier isotopic compositions are for low elevations.

Many, but not all, paleoaltimetry studies have sought to sample below 50 cm in paleosols based on theoretical and experimental observations that evaporation from the surface has minimal direct impact on soil water isotopes below this depth (Table S8) (e.g., Quade et al., 2007). However, mixing of partially evaporated near-surface soil water with infiltrating precipitation promotes indirect enrichment of heavy isotopes in deeper soil waters (Breecker et al., 2009; Mathieu and Bariac, 1996). Observations in arid soils indicate that soil waters deeper than 50 cm can be up to $\sim$7‰ heavier in $\delta^{18}O_w$ than annual mean $\delta^{18}O_p$ (Breecker et al., 2009; Hsieh et al., 1998). Thus, soil waters below the 50 cm threshold may still exhibit evaporative bias relative to mean annual δ_p. Alternating 3–4 day periods of sun followed by convective rain are typical during the central Andes rainy season (Garreaud et al., 2003). This intermittent precipitation on the Altiplano during the rainy season allows for surficial waters to evaporate between storms. These evaporated surface waters may mix with subsequent rains, which would push partially evaporated waters to lower depths in the soil, and bias soil water isotopic compositions to heavier values than precipitation.

If we assume δ_w reflects the composition of surficial soil waters, we can make an order-of-magnitude estimate of the evaporative bias in deeper soil waters. We assume that the soil water in carbonate forming horizons is a mix of 70% unevaporated precipitation and 30% shallow, evaporated soil waters. This partitioning is based on observations from African soils in a similar hydroclimate (Mathieu and Bariac, 1996). For example, surface water shifts of 2.0 and 5.0‰ relative to precipitation would result in soil waters in carbonate forming horizons that are 0.6–1.5‰ more positive than $\delta^{18}O_p$. Based on modern precipitation lapse rates (Fiorella et al., 2015; Gonfiantini et al., 2001), carbonates forming from these soil waters would record compositions associated with ~1 km lower surface elevations due solely to the isotopic offset between precipitation and soil water (Table 1). The magnitude of this bias depends on the fraction of surficial waters mixing with deeper soil waters, which in turn, depends on soil properties, climate, and vegetation (Mathieu and Bariac, 1996). Soils where more (less) than 30% of total soil water in carbonate forming horizons from evaporated shallow soil waters will exhibit a larger (smaller) evaporative bias. Changes in soil properties through time may be difficult to determine, but paleoclimate model simulations can constrain changes in the net evaporation through time.

5.2. Intensity and seasonality of net evaporation during uplift

Several lines of geological evidence, in addition to climate model results, support arid conditions in the ancient central Andes. Evaporite sequences are observed in adjacent Atacama sediments from the end Triassic onward (e.g., Clarke, 2006). In the Altiplano, evaporites are observed from ~15 Ma, and have been taken as evidence for the development of internal drainage (Alonso et al., 1991; Vandervoort et al., 1995). The absence of evaporates prior to ~15 Ma may therefore reflect that the Altiplano was an externally drained basin, and does not necessarily suggest the region was less arid prior to this time. The central Andes lie in the dry subtropics, where moisture convergence and precipitation formation are inhibited by strong atmospheric subsidence. South America has not changed latitude significantly since the Triassic (e.g., Gurnis et al., 2012), and therefore, the central Andes have been in a region of strong atmospheric subsidence throughout the Cenozoic. Andean uplift promotes the development and strengthening of the South American Low Level Jet, increasing moisture convergence and precipitation on the eastern flank of the central Andes, and resulting in less arid conditions (Insel et al., 2010). Ultimately, a higher E/P ratio early in the uplift of the Andes implies a larger magnitude evaporative bias in more ancient proxy materials.

Surface uplift also changes the seasonality of aridity, which we expect to change the seasonal timing of pedogenic carbonate formation (Fig. 7) (e.g., Peters et al., 2013). This change in carbonate formation timing will influence both the $\delta^{18}O_{cc}$ value and the formation temperature inferred from clumped isotope thermometry (Δ_{47} compositions for pedogenic carbonates). Dry conditions that follow the rainy season in the central Andes during austral fall and winter likely instigate modern pedogenic carbonate formation. However, paleoclimate models suggest a later termination of the rainy season when the Andes are at low elevations ($\leq$25% of modern), with evapotranspiration rates exceeding precipitation rates starting in May compared to April when the mountains are higher (Fig. 7a). This result suggests that when plateau elevations were lower, carbonate formation was shifted later in the year. However, this effect was unlikely to be uniform throughout the Altiplano, as the transition to an earlier onset of the dry season associated with uplift is less pronounced north of 17°S (Fig. 7b), and more pronounced south of 17°S (Fig. 7c, d). As both soil temperature and $\delta^{18}O_w$ contribute to $\delta^{18}O_{cc}$, the shift to earlier carbonate formation would bias $\delta^{18}O_{cc}$ and Δ_{47} toward summer temperatures and $\delta^{18}O_w$.

Finally, the number of annual carbonate precipitation periods may have changed during Andean surface uplift. The modern evapotranspiration rate exceeds the precipitation amount for a single extended period (April–September). A similar pattern is observed when the Andes are at least 50% of their modern elevations (Fig. 7a). Thus, pedogenic carbonates would form only during April–September when the Andes exceed 50% of modern elevations. In contrast, when the Andes are below 50% of their modern elevations, evapotranspiration exceeds precipitation both before (e.g., October–December) and after the rainy season (e.g., May–August), suggesting two distinct periods of possible carbonate growth. With two seasons of carbonate formation, the bulk carbonate composition would record a mixture of both dry and rainy season soil waters and soil temperatures. Modern precipitation during the dry season can exhibit $\delta^{18}O_p$ that is >5‰ more positive than rainy season $\delta^{18}O_p$ (Fiorella et al., 2015; Gonfiantini et al., 2001). Using the same logic as above to estimate soil water $\delta^{18}O$, dry season soil waters would be >1.5‰ more positive than rainy season soil waters. Applying modern isotopic lapse rates to this difference in seasonal soil water compositions indicates that pedogenic carbonates forming in equilibrium with dry season soil waters would further underestimate elevations by ~1 km. Additionally, if carbonate precipitation occurs during both the summer and winter while elevations are low before transitioning to winter-only formation when elevations are high, low elevation samples will be biased to lower Δ_{47} values, resulting in artificially warm temperatures. This reflects both the higher formation temperatures during the summer and due to non-linear effects in Δ_{47} values resulting from the homogenization of summer and winter carbonate values during analysis (Defliese and Lohmann, 2015).

5.3. Implications for central Andes paleoaltimetry

Stable isotope compositions of central Andes proxy materials have been used to support interpretations of rapid, punctuated, and spatially variable uplift, including uplift magnitudes of: (a) 2.2–3.7 km between 19–16 Ma for the Peruvian Western Cordillera (Saylor and Horton, 2014), (b) 2.5 ± 1.0 km between 10.3–6.8 Ma for the Bolivian Altiplano (Garzione et al., 2006), and (c) 2.5–4.0 km since 29 Ma for the Eastern Cordillera (Leier et al., 2013). These high magnitudes and short durations of uplift stand in contrast with other lines of evidence including structural observations of: (a) crustal thicknesses of ~50–60 km for the Altiplano and Eastern Cordillera during the Oligocene (McQuarrie, 2002), (b) a strong association between crustal thickening and tectonic shortening at these latitudes (~17–21°S) (Kley and Monaldi, 1998), and (c) consistent regional shortening rates of 8–10 mm/yr from ~40 Ma (Barnes and Ehlers, 2009). Furthermore, deformation in the Eastern Cordillera and Altiplano precedes apparent uplift by >10 Ma (Horton et al., 2001; Lamb and Hoke, 1997).

These differences between the surface uplift and deformation histories can be explained by isotopic fractionation associated with climate change during surface uplift (Ehlers and Poulsen, 2009; Insel et al., 2012; Poulsen et al., 2010; Poulsen and Jeffery, 2011). Thus, proxy isotopic compositions may not only record changes in elevation, but also changes in climate. Proxy material isotopic compositions exhibit large variability within and between study sites (Fig. 8, Garzione et al., 2014, 2008; Leier et al., 2013; Saylor and Horton, 2014). Carbonates deposited from 6–7 Ma in the Corque Syncline show $\delta^{18}O_{cc}$ values ranging from −15.3 to −8.3‰ (Fig. 8, Garzione et al., 2006). Likewise, though no values heavier than ~−110‰ for δD occur in hydrated volcanic glass compositions after ~17 Ma in the Condoroma Basin in Peru

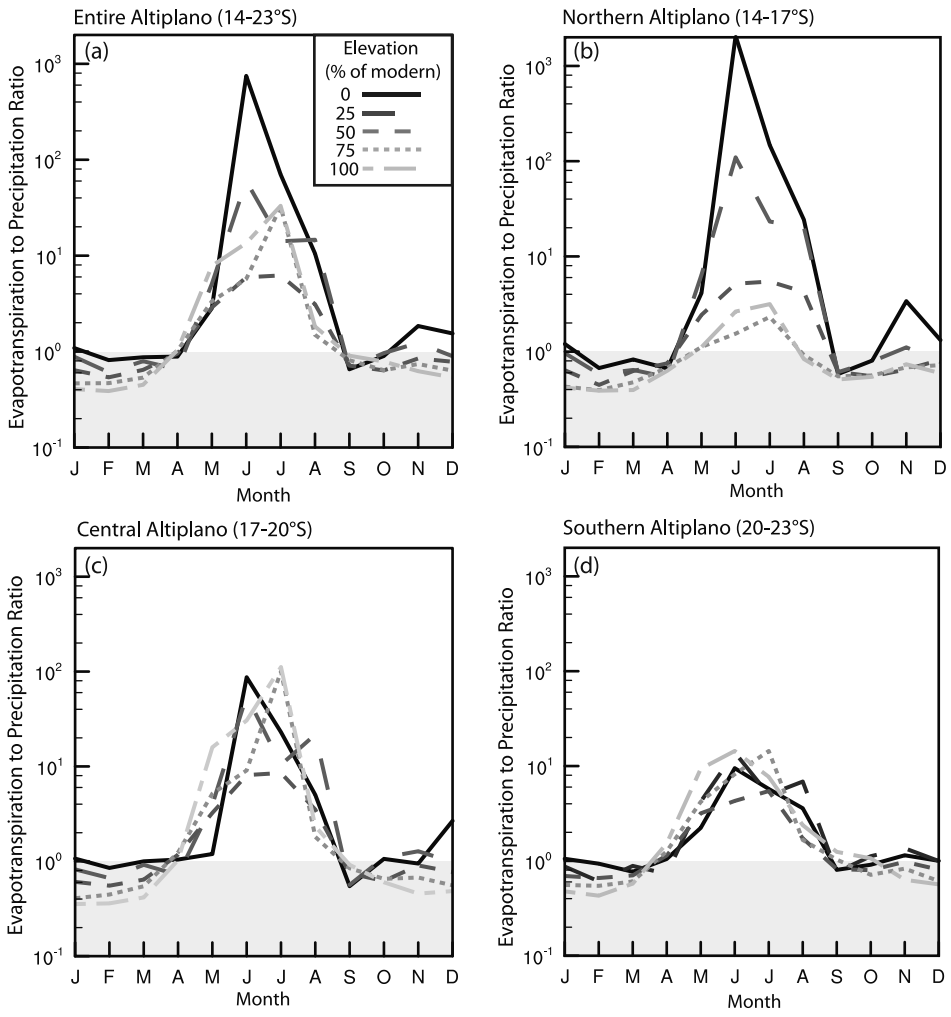

Fig. 7. Monthly evapotranspiration to precipitation ratios for each climate model scenario for the entire Altiplano (a, 14–23°S), the northern Altiplano (b, 14–17°S), the central Altiplano (c, 17–20°S), and the southern Altiplano (d, 20–23°S). At higher elevations (>50%), evapotranspiration exceeds precipitation from April to September. In contrast, at lower elevations (<50%), evapotranspiration exceeds precipitation during two distinct periods (May–August, October–December). These changes in the annual hydrologic budget imply that the timing of pedogenic carbonate formation may have changed throughout the uplift and complicates direct comparison of $\delta^{18}O_{cc}$ values from different periods of Andes uplift.

(Saylor and Horton, 2014), isotopic compositions vary by at least ~70‰ in samples with overlapping dating uncertainty.

Variability between these sites has been interpreted to reflect relative uplift between sites, perhaps by as much as multiple kilometers. Alternatively, this variability may represent changes in the spatial pattern of evaporation between sites. Proxy materials formed from evaporated waters would record heavier isotopic compositions associated with lower elevations. Based on climate modeling patterns of precipitation and evapotranspiration, this isotopic bias increases for more ancient proxy materials when elevations were lower. To minimize the impact of evaporative bias in paleoaltimetry studies, it has been suggested that only the lightest isotopic compositions should be used to reconstruct elevations (e.g., Rowley and Currie, 2006). However, this maxim has been inconsistently applied to central Andes stable isotope paleoaltimetry studies.

Here, we reconsider the Bolivian Altiplano and Eastern Cordillera paleoaltimetry record using only the most negative isotopic compositions available. Starting with the Corque syncline on the Bolivian Altiplano, we identify four key carbonate compositions to construct a paleoelevation history based on the lightest isotopic compositions: −12.1‰ at 24.5 Ma, −13.3‰ at 11.45 Ma, −14.1‰ at 7.35 Ma, and −15.1‰ at 6.74 Ma (VPDB) (Garzione et al., 2008). The composition of meteoric water in equilibrium with these carbonates can be estimated by applying temperature constraints to the temperature-dependent fractionation of oxygen between calcite and water (Kim and O'Neil, 1997). Assuming formation temperatures of 36 °C, 28 °C, 18 °C, and 13 °C based on clumped isotope paleothermometry (Ghosh et al., 2006; Leier et al., 2013), these carbonate compositions imply meteoric water compositions of −7.6‰ at 24.5 Ma, −10.3‰ at 11.45 Ma, −13.2‰ at 7.35 Ma, and −16.2‰ at 6.74 Ma (VSMOW). An annual mean $\delta^{18}O_p$ of −7.6‰ is inconsistent with near sea-level elevations, but is consistent with Andean elevations of ~25–50% of modern, or 1.0–2.0 km (Insel et al., 2012). Additionally, the $\delta^{18}O_p$ estimated for 6.74 Ma is consistent with modern observations (Fiorella et al., 2015; Gonfiantini et al., 2001), suggesting that modern elevations were reached by this time. This result limits the total Altiplano uplift after 24.5 Ma to 1.7–3.0 km. Partitioning the 8.6‰ of estimated $\delta^{18}O_p$ change proportionally between these four points suggests uplift magnitudes of: 0.5–1.0 km from 24.5–11.45 Ma, 0.6–1.0 km from 11.45–7.35 Ma, and 0.6–1.0 km from 7.35–6.74 Ma. These uplift magnitudes would imply plateau elevations of 1.0–2.0 km at 24.5 Ma, and >1.5 km by 11.45 Ma and >2.1 km by 7.35 Ma (Fig. 9a). Therefore, the total uplift of the Altiplano after 11.45 Ma cannot exceed ~2.2 km, and may have been as small as ~0.7 km. These estimates are substantially smaller than previous interpretations of the isotopic data of 2.5 ± 1.0 km of uplift after 11.45 Ma

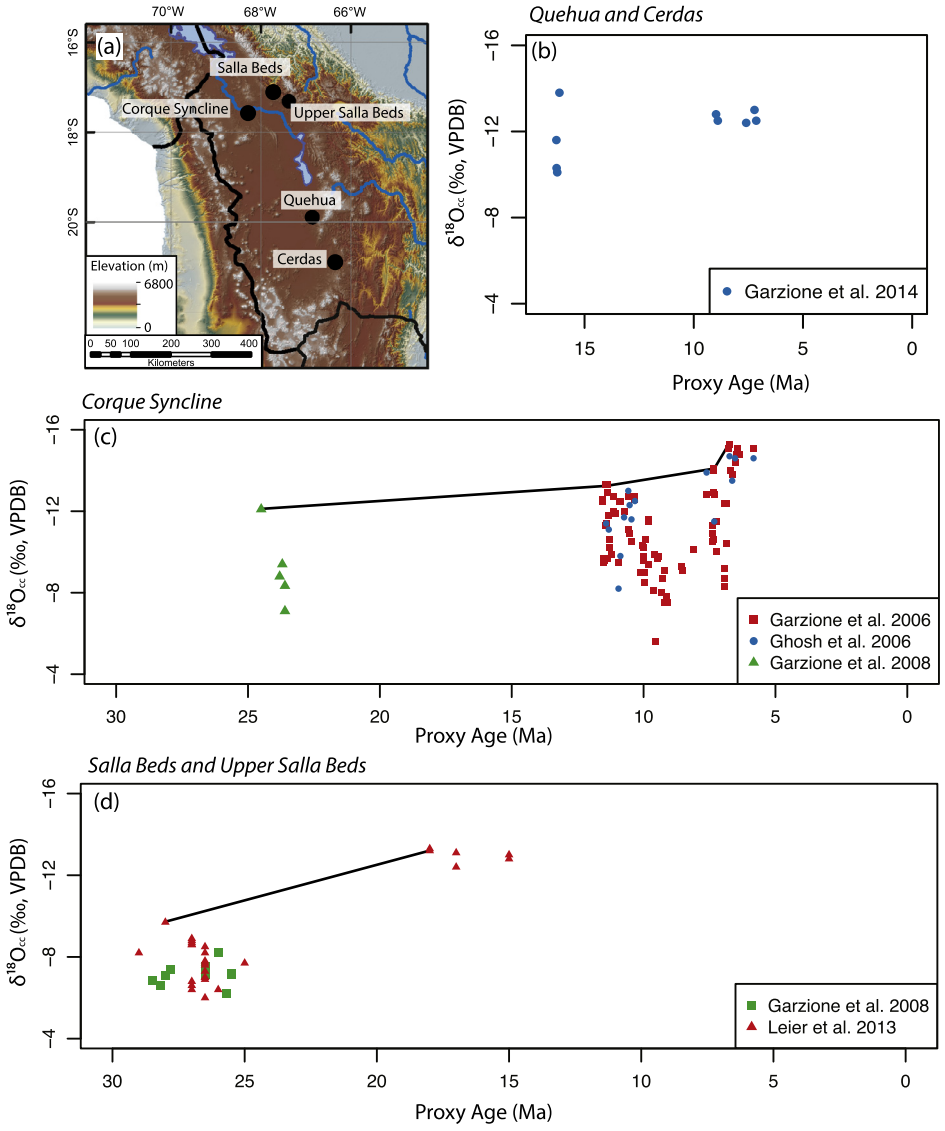

Fig. 8. Proxy material sampling locations (a) and compilation of available proxy $\delta^{18}O_{cc}$ values from the central Andes plotted against proxy age for (b) Quehua and Cerdas (Garzione et al., 2014), (c) the Corque Syncline (Garzione et al., 2006, 2008; Ghosh et al., 2006) and (d) the Salla and Upper Salla Beds (Garzione et al., 2008; Leier et al., 2013). Data points used in our proposed reconstruction using only the most negative carbonate values are connected in (c) and (d) with thin black lines.

(e.g., Garzione et al., 2008). Further, our estimates represent maximum uplift magnitudes and place minimum bounds on past elevations, if the following two assumptions are correct: (1) the lightest isotopic compositions capture unevaporated meteoric water and (2) the isotopic composition of this proxy material represents the multi-year mean of the precipitation composition. In arid climates, compositions reflecting unevaporated water may not be preserved (Quade et al., 2007), and therefore, elevations may be higher than suggested by the most negative proxy composition. Finally, we note that our assumption that clumped isotope compositions accurately record the proxy formation temperature is the more conservative approach to reinterpret the $\delta^{18}O_{cc}$ data with respect to the original interpretations. If RegCM surface temperatures were used to estimate $\delta^{18}O_p$ instead, the estimated change in $\delta^{18}O_p$ would drop to a maximum of 7.7‰ instead of 8.6‰, which would also suggest a lower uplift magnitude. Furthermore, a formation temperature of 28 °C from RegCM at 24.5 Ma implies a $\delta^{18}O_p$ of −9.1‰, and potentially higher paleoelevations than the 1–2 km estimated here.

Surface temperature histories inferred from clumped isotope compositions of pedogenic carbonates suggest that the southern Bolivian Altiplano was uplifted by 2.5 ± 1.0 km between 16 and 13 Ma. In contrast, clumped isotope temperatures indicate the northern Bolivian Altiplano remained below 2 km until ∼10 Ma, and experienced 2.5 ± 1.0 km of uplift between 10 and 6 Ma (Garzione et al., 2014; Ghosh et al., 2006). However, the most negative $\delta^{18}O$ compositions from the north and south halves of the Bolivian Altiplano do not show this discrepancy. The lightest isotopic compositions at the Cerdas and Quehua sites in the southern Altiplano are −13.8‰ at 16.15 Ma and −13.0‰ at 7.22 Ma respectively, while compositions of −12.1‰ at 24.5 Ma and −14.1‰ at 7.35 Ma are observed at the Corque Syncline (Fig. 8). Therefore, $\delta^{18}O$ compositions would seem to suggest a spatially uniform uplift of the Bolivian Altiplano, in contrast to the heterogeneous uplift history previously inferred from Δ_{47} compositions. However, clumped isotope temperature estimates are highly uncertain for portions of the central Andes record. For example, carbonates within the Corque Syncline show a ∼25 °C range of temperature at 11 Ma and a ∼20 °C range of temperature at 6 Ma, while the Salla Beds also show a ∼25 °C range at 25 Ma (Fig. S3, Garzione et al., 2008; Leier et al., 2013). The RegCM temperature change between the 0% and 100% Andes simulations is ∼22 °C. Therefore, the temperature uncertainty for contemporaneously precipitated pedo-

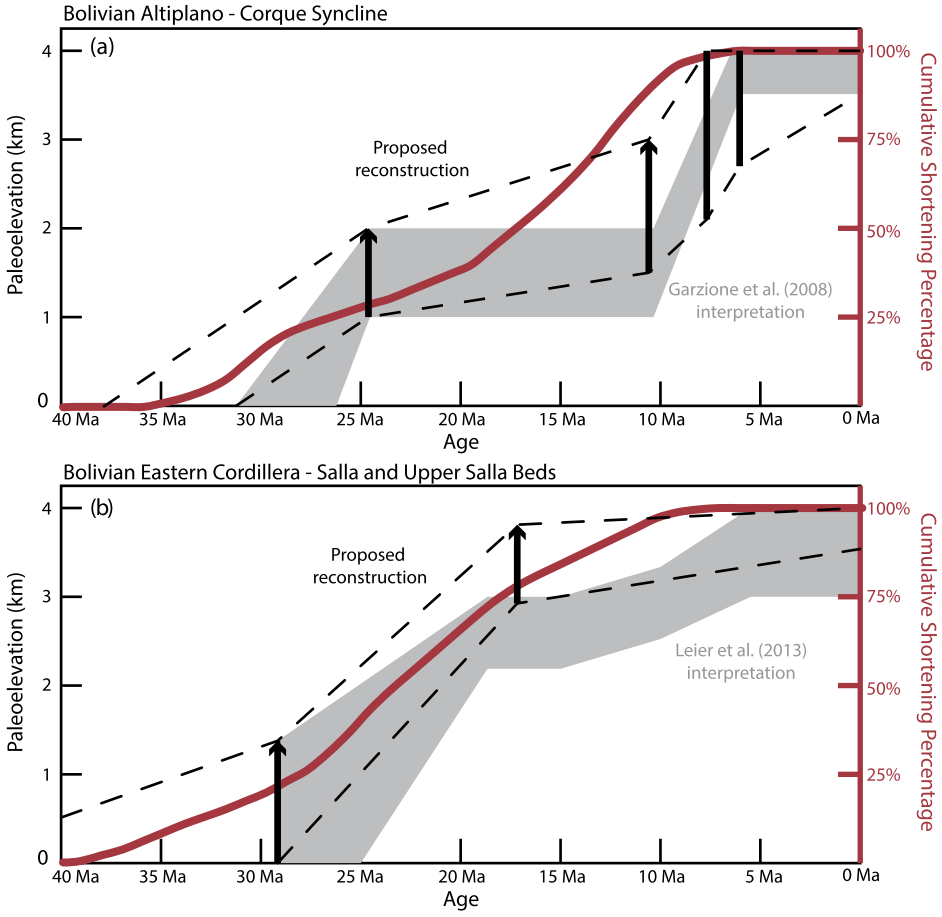

Fig. 9. Schematic of the uplift of the Bolivian Altiplano (a) and Eastern Cordillera (b) proposed in this study. Key isotopic constraints identified in Section 5.3 are shown in thick black lines, with arrows indicating that higher elevations are possible if a pedogenic carbonate in equilibrium with precipitation was not preserved. The range of elevations suggested by using only the lightest $\delta^{18}O_{cc}$ compositions in the proxy record is outlined in dashed black lines, though we note other uplift paths through the constraints identified are possible. Previous interpretations of the stable isotope data are shown in gray. Cumulative shortening after Oncken et al. (2006) is shown for each region as a red curve. For both regions, the proposed post-15 Ma uplift is reduced from the original interpretations, and provides a closer match between cumulative shortening and reconstructed elevations. (For interpretation of the references to color in this figure legend, the reader is referred to the web version of this article.)

genic carbonates approaches the anticipated signal for the entire uplift of the Andes. As such, the clumped isotope record places weaker constraints on the paleoelevation history of the central Andes than do $\delta^{18}O$ compositions. As a result, our proposed Altiplano uplift scenario remains consistent with clumped isotope temperatures (SI results). This trend arises from the large Δ_{47} temperature variability as well as from uncertainties in the relationship between Δ_{47} formation temperatures and mean annual air temperatures (SI discussion).

Therefore, based on our prior assertion that more negative isotopic compositions are stronger evidence for high elevations than less negative compositions are for low elevations, we suggest that broadly synchronous uplift of the Bolivian Altiplano is consistent with the $\delta^{18}O_{cc}$ data (Fig. S3). In addition, Δ_{47} temperatures also suggest a homogeneous uplift of the Bolivian Altiplano when temperature estimates for Corque, Cerdas, and Quehua are estimated using the model of Quade et al. (2013, and see SI results, Fig. S3). Broadly synchronous uplift is also supported by evidence of similar deformation histories in the northern (Lamb and Hoke, 1997) and southern (Elger et al., 2005) portions of the Bolivian Altiplano. Additionally, recent isotopic evidence suggests that the Puna plateau may have attained modern elevations at least as early as the mid-Miocene (e.g., Quade et al., 2015), and perhaps as early as the Eocene (Canavan et al., 2014). Taken together, we suggest that a broadly uniform uplift of the entire central Andean plateau may yet be consistent with the isotopic data due to the strong hydrologic changes associated with uplift that may be reflected in proxy isotope compositions. Further, our proposed paleoelevation history is more consistent with crustal shortening records for the Altiplano (Eichelberger et al., 2015; Elger et al., 2005; Lamb and Hoke, 1997; Oncken et al., 2006), and does not require massive, large-scale delamination.

In the Eastern Cordillera, the most negative $\delta^{18}O_{cc}$ value for the Salla Beds is −9.7‰ at 28.0 Ma, and −13.9‰ at 18.0 Ma for the Upper Salla Beds (VPDB) (Leier et al., 2013). Assuming formation temperatures (from Δ_{47}) of $36 \pm 4\,^{\circ}C$ for the Salla Beds and $20 \pm 3\,^{\circ}C$ for the Upper Salla Beds yields estimates of $\delta^{18}O_p$ of -5.0 ± 0.7‰ and -12.5 ± 0.6‰ for the Salla and Upper Salla Beds respectively (VSMOW). This estimate of $\delta^{18}O_p$ for the Salla Beds is slightly more negative than the estimation of Leier et al. (2013) of −4.0‰, but remains consistent with their interpretation of Salla Bed paleoelevations of 0–1.5 km (Fig. 9b). In contrast, a value of -12.5 ± 0.6‰ for $\delta^{18}O_p$ during deposition of the Upper Salla Beds suggests surface elevations >3 km (Fig. 9b). Modern water isotope values more depleted than −12.0‰ are not observed in precipitation and stream waters below 3 km (Bershaw et al., 2010; Fiorella et al., 2015; Gonfiantini et al., 2001). Furthermore, isotope tracking climate model experiments also indicate that $\delta^{18}O_p$ values less than −12.0‰ require elevations of >3 km (Insel et al., 2012). Therefore, we suggest the Upper Salla Beds were deposited above 3 km. This is consistent with the estimate of 3.2 ± 0.5 km in Leier et al. (2013) when all carbonate values are included, but

inconsistent with their elevation estimate of ~2.5 km when the most negative carbonate value is treated as an outlier.

Finally, though we have considered evaporation in isolation, changes in Cenozoic climate have also likely impacted proxy isotopic compositions as well as evaporative intensity. Globally warmer conditions in the Paleogene relative to the Neogene may amplify evaporative bias (e.g., Zachos et al., 2001). Additionally, enhanced atmospheric subsidence would be expected over the central Andes region in a warmer climate. This atmospheric subsidence would transport heavier-than-anticipated vapor to the surface, and further bias proxy materials to lower elevations (Poulsen and Jeffery, 2011). Unfortunately, the magnitude of evaporative bias is difficult to constrain throughout time in the absence of quantitative proxy-based estimates of net evaporation. We suggest that recent developments in ^{17}O-excess, an isotopic marker which records evaporative intensity when combined with $\delta^{18}O_{cc}$, may represent an important step forward to decoupling the contributions of climate and tectonic change to isotopic change (e.g., Passey et al., 2014).

6. Conclusions

We provide a dataset of the isotopic composition of 249 central Andes streams collected over a 3.5-year period, constraining an important and previously missing aspect of the central Andes stable isotope system. The isotopic compositions of stream waters along the eastern Andean flank possess a δD–δ^{18}O that is similar to regional precipitation. In contrast, stream waters on the Altiplano exhibit a δD–δ^{18}O relationship with a shallower slope than that of regional precipitation, which we interpret as evidence of heavy isotope enrichment through evaporation. Propagation of this evaporative signal into soil waters that occurs during infiltration may result in soil water and carbonate compositions that underestimate modern elevations in modern soils. Paleoclimate model simulations indicate that the central Andes region has become progressively less arid through its uplift, and therefore, carbonates earlier in the uplift history may exhibit a greater bias. Cenozoic cooling and the increase in isotopic lapse rates inferred from climate modeling both amplify this bias (Insel et al., 2012; Jeffery et al., 2012; Poulsen et al., 2010; Poulsen and Jeffery, 2011).

To avoid this bias, we propose paleoelevations for the Bolivian Altiplano of 1–2 km at 24.5 Ma, 1.5–3.0 km at ~11.45 Ma, and 2.7–4 km at 6 Ma based on the lightest isotopic compositions observed in proxy materials. Using the same logic, we estimate paleoelevations for the Eastern Cordillera of 0–1.5 km at ~28 Ma and >3 km at ~18 Ma. We draw three major conclusions from this reinterpretation of stable isotope proxy data: (1) mid-Miocene-to-modern elevation change on the Bolivian Altiplano was no greater than 2 km, which is less than prior stable isotope based estimates of 2.5 ± 1 km (Garzione et al., 2008, 2014), (2) Bolivian Altiplano and Eastern Cordillera paleoelevations inferred in this study more closely match records of cumulative shortening (Fig. 9) (Barnes and Ehlers, 2009; Oncken et al., 2006) than do prior interpretations of stable isotope data, (3) when placed into a consistent framework, δ^{18}O and Δ_{47} compositions support a uniform, homogeneous uplift of the Bolivian Altiplano. Therefore, central Andes surface uplift may be more spatially uniform and more closely linked to crustal shortening than suggested in previous interpretations of stable isotope paleoelevation proxies.

Acknowledgements

RPF received an NSF Graduate Research Fellowship Grant 2011094378, and a Rackham International Research Grant from the Rackham Graduate School at the University of Michigan (UM). RPF and MLJ received support from Turner Graduate Student Research Grants from the UM Department of Earth and Environmental Sciences. CJP and TAE received support from NSF EAR Grants 0738822 and 0907818; CJP also received support through the UM Associate Professor Fund. We thank J. Tito, G. Gonzalez, S. Tawackoli, C.R. Tabor, J.B. Barnes, N. Insel, and M. Tracy for assistance in the field. The authors thank J.E. Saylor, an anonymous reviewer, and editor A. Yin for comments that improved this manuscript.

Appendix A. Supplementary material

Supplementary material related to this article can be found online at http://dx.doi.org/10.1016/j.epsl.2015.09.045.

References

Alonso, R.N., Jordan, T.E., Tabbutt, K.T., Vandervoort, D.S., 1991. Giant evaporite Belts of the Neogene Central Andes. Geology 19, 401–404. http://dx.doi.org/10.1130/0091-7613(1991)019<0401:GEBOTN>2.3.CO;2.

Aravena, R., Suzuki, O., Pena, H., Pollastri, A., Fuenzalida, H., Grilli, A., 1999. Isotopic composition and origin of the precipitation in Northern Chile. Appl. Geochem. 14, 411–422. http://dx.doi.org/10.1016/S0883-2927(98)00067-5.

Barnes, J.B., Ehlers, T.A., 2009. End member models for Andean Plateau uplift. Earth-Sci. Rev. 97, 105–132. http://dx.doi.org/10.1016/j.earscirev.2009.08.003.

Bershaw, J., Garzione, C.N., Higgins, P., MacFadden, B.J., Anaya, F., Alvarenga, H., 2010. Spatial–temporal changes in Andean plateau climate and elevation from stable isotopes of mammal teeth. Earth Planet. Sci. Lett. 289, 530–538. http://dx.doi.org/10.1016/j.epsl.2009.11.047.

Breecker, D.O., Sharp, Z.D., McFadden, L.D., 2009. Seasonal bias in the formation and stable isotopic composition of pedogenic carbonate in modern soils from central New Mexico, USA. Geol. Soc. Am. Bull. 121, 630–640. http://dx.doi.org/10.1130/B26413.1.

Canavan, R.R., Carrapa, B., Clementz, M.T., Quade, J., DeCelles, P.G., Schoenbohm, L.M., 2014. Early Cenozoic uplift of the Puna Plateau, Central Andes, based on stable isotope paleoaltimetry of hydrated volcanic glass. Geology 42, 447–450. http://dx.doi.org/10.1130/G35239.1.

Clarke, J.D.A., 2006. Antiquity of aridity in the Chilean Atacama Desert. Geomorphology 73, 101–114. http://dx.doi.org/10.1016/j.geomorph.2005.06.008.

Coplen, T.B., 1996. New guidelines for reporting stable hydrogen, carbon, and oxygen isotope-ratio data. Geochim. Cosmochim. Acta 60, 3359–3360. http://dx.doi.org/10.1016/0016-7037(96)00263-3.

Defliese, W.F., Lohmann, K.C., 2015. Non-linear mixing effects on mass-47 CO_2 clumped isotope thermometry: patterns and implications. Rapid Commun. Mass Spectrom., 1–9. http://dx.doi.org/10.1002/rcm.7175.

Ehlers, T.A., Poulsen, C.J., 2009. Influence of Andean uplift on climate and paleoaltimetry estimates. Earth Planet. Sci. Lett. 281, 238–248. http://dx.doi.org/10.1016/j.epsl.2009.02.026.

Eichelberger, N., McQuarrie, N., Ryan, J., Karimi, B., Beck, S., Zandt, G., 2015. Evolution of crustal thickening in the central Andes, Bolivia. Earth Planet. Sci. Lett. 426, 191–203. http://dx.doi.org/10.1016/j.epsl.2015.06.035.

Elger, K., Oncken, O., Glodny, J., 2005. Plateau-style accumulation of deformation: Southern Altiplano. Tectonics 24. http://dx.doi.org/10.1029/2004TC001675.

Fiorella, R.P., Poulsen, C.J., Pillco Zolá, R.S., Barnes, J.B., Tabor, C.R., Ehlers, T.A., 2015. Spatiotemporal variability of modern precipitation δ^{18}O in the central Andes and implications for paleoclimate and paleoaltimetry estimates. J. Geophys. Res., Atmos. 120, 4630–4656. http://dx.doi.org/10.1002/2014JD022893.

Garreaud, R.D., Vuille, M., Clement, A., 2003. The climate of the Altiplano: observed current conditions and mechanisms of past changes. Palaeogeogr. Palaeoclimatol. Palaeoecol. 194, 5–22. http://dx.doi.org/10.1016/S0031-0182(03)00269-4.

Garzione, C.N., Auerbach, D.J., Smith, J.J.-S., Rosario, J.J., Passey, B.H., Jordan, T.E., Eiler, J.M., 2014. Clumped isotope evidence for diachronous surface cooling of the Altiplano and pulsed surface uplift of the Central Andes. Earth Planet. Sci. Lett. 393, 173–181. http://dx.doi.org/10.1016/j.epsl.2014.02.029.

Garzione, C.N., Hoke, G.D., Libarkin, J.C., Withers, S., MacFadden, B.J., Eiler, J.M., Ghosh, P., Mulch, A., 2008. Rise of the Andes. Science 320, 1304–1307. http://dx.doi.org/10.1126/science.1148615.

Garzione, C.N., Molnar, P., Libarkin, J.C., MacFadden, B.J., 2006. Rapid late Miocene rise of the Bolivian Altiplano: evidence for removal of mantle lithosphere. Earth Planet. Sci. Lett. 241, 543–556. http://dx.doi.org/10.1016/j.epsl.2005.11.026.

Ghosh, P., Garzione, C.N., Eiler, J.M., 2006. Rapid uplift of the Altiplano revealed through ^{13}C–^{18}O bonds in paleosol carbonates. Science 311, 511–515. http://dx.doi.org/10.1126/science.1120792.

Gonfiantini, R., Roche, M.A., Olivry, J.C., Fontes, J.C., Zuppi, G.M., 2001. The altitude effect on the isotopic composition of tropical rains. Chem. Geol. 181, 147–167.

Gurnis, M., Turner, M., Zahirovic, S., DiCaprio, L., Spasojevic, S., Müller, R.D., Boyden, J., Seton, M., Manea, V.C., Bower, D.J., 2012. Plate tectonic reconstructions with continuously closing plates. Comput. Geosci. 38, 35–42. http://dx.doi.org/10.1016/j.cageo.2011.04.014.

Horton, B.K., Hampton, B.A., Waanders, G.L., 2001. Paleogene synorogenic sedimentation in the Altiplano plateau and implications for initial mountain building in the central Andes. Geol. Soc. Am. Bull. 113, 1387–1400. http://dx.doi.org/10.1130/0016-7606(2001)113<1387:PSSITA>2.0.CO;2.

Hsieh, J., Chadwick, O.A., Kelly, E.F., Savin, S.M., 1998. Oxygen isotopic composition of soil water: quantifying evaporation and transpiration. Geoderma 82, 269–293.

Insel, N., Poulsen, C.J., Ehlers, T.A., 2010. Influence of the Andes Mountains on South American moisture transport, convection, and precipitation. Clim. Dyn. 35, 1477–1492. http://dx.doi.org/10.1007/s00382-009-0637-1.

Insel, N., Poulsen, C.J., Ehlers, T.A., Sturm, C., 2012. Response of meteoric $\delta^{18}O$ to surface uplift – implications for Cenozoic Andean plateau growth. Earth Planet. Sci. Lett. 317–318, 262–272. http://dx.doi.org/10.1016/j.epsl.2011.11.039.

Isacks, B.L., 1988. Uplift of the Central Andean plateau and bending of the Bolivian orocline. J. Geophys. Res. 93, 3211–3231.

Jeffery, M.L., Poulsen, C.J., Ehlers, T.A., 2012. Impacts of Cenozoic global cooling, surface uplift, and an inland seaway on South American paleoclimate and precipitation $\delta^{18}O$. Geol. Soc. Am. Bull. 124, 335–351. http://dx.doi.org/10.1130/B30480.1.

Kendall, C., Coplen, T.B., 2001. Distribution of oxygen-18 and deuterium in river waters across the United States. Hydrol. Process. 15, 1363–1393. http://dx.doi.org/10.1002/hyp.217.

Kim, S.-T., O'Neil, J.R., 1997. Equilibrium and nonequilibrium oxygen isotope effects in synthetic carbonates. Geochim. Cosmochim. Acta 61, 3461–3475. http://dx.doi.org/10.1016/S0016-7037(97)00169-5.

Kley, J., Monaldi, C.R., 1998. Tectonic shortening and crustal thickness in the Central Andes: how good is the correlation? Geology 26, 723–726. http://dx.doi.org/10.1130/0091-7613(1998)026<0723:TSACTI>2.3.CO;2.

Lamb, S., Hoke, L., 1997. Origin of the high plateau in the Central Andes, Bolivia, South America. Tectonics 16, 623–649.

Leier, A., McQuarrie, N., Garzione, C., Eiler, J., 2013. Stable isotope evidence for multiple pulses of rapid surface uplift in the Central Andes, Bolivia. Earth Planet. Sci. Lett. 371–372, 49–58. http://dx.doi.org/10.1016/j.epsl.2013.04.025.

Mathieu, R., Bariac, T., 1996. An isotopic study (^2H and ^{18}O) of water movements in clayey soils under a semiarid climate. Water Resour. Bull. 32, 779–789.

McQuarrie, N., 2002. The kinematic history of the central Andean fold-thrust belt, Bolivia: implications for building a high plateau. Geol. Soc. Am. Bull. 114, 950–963. http://dx.doi.org/10.1130/0016-7606(2002)114<0950:TKHOTC>2.0.CO;2.

McQuarrie, N., Horton, B.K., Zandt, G., Beck, S., DeCelles, P.G., 2005. Lithospheric evolution of the Andean fold–thrust belt, Bolivia, and the origin of the central Andean plateau. Tectonophysics 399, 15–37. http://dx.doi.org/10.1016/j.tecto.2004.12.013.

Mulch, A., Chamberlain, C.P., 2007. Stable isotope paleoaltimetry in orogenic belts the silicate record in surface and crustal geological archives. In: Kohn, M.J. (Ed.), Paleoaltimetry: Geochemical and Thermodynamic Approaches. Minerology Society of America, pp. 89–118.

Oncken, O., Hindle, D., Kley, J., Elger, K., Victor, P., Schemmann, K., 2006. Deformation of the Central Andean upper plate system – facts, fiction, and constraints for plateau models. In: Oncken, O., Chong, G., Franz, G., Giese, P., Götze, H.-J., Ramos, V.A., Strecker, M.R., Wigger, P. (Eds.), The Andes. Springer, Berlin, Heidelberg, pp. 3–27.

Pal, J., Giorgi, F., Bi, X., Elguindi, N., Solmon, F., Rauscher, S., Gao, X., Francisco, R., Zakey, A., Winter, J., 2007. Regional climate modeling for the developing world: the ICTP RegCM3 and RegCNET. Bull. Am. Meteorol. Soc. 88, 1395–1409. http://dx.doi.org/10.1175/BAMS-88-9-1395.

Passey, B.H., Hu, H., Ji, H., Montanari, S., Li, S., Henkes, G.A., Levin, N.E., 2014. Triple oxygen isotopes in biogenic and sedimentary carbonates. Geochim. Cosmochim. Acta 141, 1–25. http://dx.doi.org/10.1016/j.gca.2014.06.006.

Peters, N.A., Huntington, K.W., Hoke, G.D., 2013. Hot or not? Impact of seasonally variable soil carbonate formation on paleotemperature and O-isotope records from clumped isotope thermometry. Earth Planet. Sci. Lett. 361, 208–218. http://dx.doi.org/10.1016/j.epsl.2012.10.024.

Poulsen, C.J., Ehlers, T.A., Insel, N., 2010. Onset of convective rainfall during gradual late Miocene rise of the Central Andes. Science 328, 490–493. http://dx.doi.org/10.1126/science.1185078.

Poulsen, C.J., Jeffery, M.L., 2011. Climate change imprinting on stable isotopic compositions of high-elevation meteoric water cloaks past surface elevations of major orogens. Geology. http://dx.doi.org/10.1130/G32052.1.

Quade, J., Dettinger, M.P., Carrapa, B., DeCelles, P., Murray, K.E., Huntington, K.W., Cartwright, A., Canavan, R.R., Gehrels, G., Clementz, M., 2015. The growth of the central Andes, 22°S–26°S. In: Geodynamics of a Cordilleran Orogenic System: the Central Andes of Argentina and Northern Chile. In: Geological Society of America Memoirs. Geological Society of America, pp. 277–308.

Quade, J., Eiler, J.M., Daëron, M., Achyuthan, H., 2013. The clumped isotope geothermometer in soil and paleosol carbonate. Geochim. Cosmochim. Acta 105, 92–107. http://dx.doi.org/10.1016/j.gca.2012.11.031.

Quade, J., Garzione, C.N., Eiler, J.M., 2007. Paleoelevation reconstruction using pedogenic carbonates. Rev. Mineral. Geochem. 66, 53–87. http://dx.doi.org/10.2138/rmg.2007.66.3.

Rohrmann, A., Strecker, M.R., Bookhagen, B., Mulch, A., Sachse, D., Pingel, H., Alonso, R.N., Schildgen, T.F., Montero, C., 2014. Can stable isotopes ride out the storms? The role of convection for water isotopes in models, records, and paleoaltimetry studies in the central Andes. Earth Planet. Sci. Lett. 407, 187–195. http://dx.doi.org/10.1016/j.epsl.2014.09.021.

Rowley, D.B., 2007. Stable isotope-based paleoaltimetry: theory and validation. In: Kohn, M.J. (Ed.), Paleoaltimetry: Geochemical and Thermodynamic Approaches. Minerology Society of America, pp. 23–52.

Rowley, D.B., Currie, B.S., 2006. Palaeo-altimetry of the late Eocene to Miocene Lunpola basin, central Tibet. Nature 439, 677–681. http://dx.doi.org/10.1038/nature04506.

Rozanski, K., Araguas-Araguas, L., Gonfiantini, R., 1993. Isotopic patterns in modern global precipitation. In: Swart, P.K., Lohmann, K.C., Mckenzie, J., Savin, S.M. (Eds.), Climate Change in Continental Isotopic Records. American Geophysical Union, pp. 1–36.

Saylor, J.E., Horton, B.K., 2014. Nonuniform surface uplift of the Andean plateau revealed by deuterium isotopes in Miocene volcanic glass from southern Peru. Earth Planet. Sci. Lett. 387, 120–131. http://dx.doi.org/10.1016/j.epsl.2013.11.015.

Saylor, J.E., Mora, A., Horton, B.K., Nie, J., 2009. Controls on the isotopic composition of surface water and precipitation in the Northern Andes, Colombian Eastern Cordillera. Geochim. Cosmochim. Acta 73, 6999–7018. http://dx.doi.org/10.1016/j.gca.2009.08.030.

Vandervoort, D.S., Jordan, T.E., Zeitler, P.K., Alonso, R.N., 1995. Chronology of internal drainage development and uplift, Southern Puna Plateau, Argentine Central Andes. Geology 23, 145–148. http://dx.doi.org/10.1130/0091-7613(1995)023<0145:COIDDA>2.3.CO;2.

Zachos, J., Pagani, M., Sloan, L.C., Thomas, E., Billups, K., 2001. Trends, rhythms, and aberrations in global climate 65 Ma to present. Science 292, 686.